Korean J. Chem. Eng., **30**(2), 474-481 (2013)
DOI: 10.1007/s11814-012-0178-x

Solubility of carbon dioxide in ammonium-based ionic liquids: Butyltrimethylammonium bis(trifluoromethylsulfonyl)imide and methyltrioctylammonium bis(trifluoromethylsulfonyl)imide

Sang Gyu Nam and Byung-Chul Lee†

Department of Chemical Engineering and Nano-Bio Technology, Hannam University,
461-6, Jeonmin-dong, Yuseong-gu, Daejeon 305-811, Korea
(*Received 29 August 2012 • accepted 13 October 2012*)

Abstract−Solubility results of carbon dioxide (CO_2) in two ammonium-based ionic liquids, butyltrimethylammonium bis(trifluoromethylsulfonyl)imide ([N4,1,1,1][Tf_2N]) and methyltrioctylammonium bis(trifluoromethylsulfonyl)imide ([N1,8,8,8][Tf_2N]), are presented at pressures up to approximately 45 MPa and temperatures ranging from 303.15 K to 343.15 K. The solubility was determined by measuring bubble point pressures of mixtures of CO_2 and ionic liquid using a high-pressure equilibrium apparatus equipped with a variable-volume view cell. Sharp increase of equilibrium pressure was observed at high CO_2 compositions. The CO_2 solubility in ionic liquids increased with the increase of the total length of alkyl chains attached to the ammonium cation of the ionic liquids. The experimental data for the CO_2+ionic liquid systems were correlated using the Peng-Robinson equation of state.

Key words: Solubility, Carbon Dioxide, Ionic Liquid, Ammonium, Correlation, Peng-Robinson Equation of State

INTRODUCTION

Ionic liquids have shown excellent performance advancing existing technologies in a variety of chemical processes, resulting in explosive expansion of research and application. Currently, they are being used as catalysts and solvents in organic or inorganic reactions, electrolytes for fuel cells, solar cells and secondary batteries, and solvents for biomass processing [1-3]. Besides their use as potential new green solvents or reaction media, ionic liquids also can be used as separation media for various separation processes, especially as absorbents for capturing CO_2 from gas mixtures [4-10]. Studies on treatment of gases through the use of ionic liquids have drawn a great attention. The nonvolatility of ionic liquids would not contaminate a gas stream, which gives ionic liquids a strong advantage over conventional solvents used for absorbing gases. To select an efficient ionic liquid for use as a gas separation medium, it is necessary to know the solubility of the gas in the ionic liquid phase. A large number of publications on the solubility of CO_2 in pure ionic liquids have been released [11-22]. Many investigators have reported that the characteristic of CO_2 absorption of ionic liquids is very useful in separating CO_2 from natural and exhaust gases. As a result, the utilization of ionic liquids for CO_2 capture and separation has recently gained great interest in the issues of global warming and CO_2 emissions [23].

The current leading technology involves CO_2 absorption by aqueous amine solutions as chemical absorbents. Even though the amine-based methods are highly efficient for CO_2 capture, they have several concerns, including high volatility, thermal instability, high energy consumption for regeneration, corrosion, and degradation of amines. Many studies on the use of ionic liquids as an alternative CO_2 absorbent, which are capable of overcoming those problems, have been conducted [8,24]. An ideal CO_2 absorbent needs to satisfy the following primary requirements: high CO_2 absorption capacity and selectivity, mild regeneration condition, thermal and chemical stability, low viscosity, and low price. As the ionic liquid consists of cation and anion, it is possible to change their characteristics by modifying the structures of cation and anion groups.

In this work, we used a high-pressure equilibrium apparatus with a variable-volume view cell to measure the CO_2 solubilities for two kinds of ammonium-based ionic liquids with the same anion: butyltrimethylammonium bis(trifluoromethylsulfonyl)imide ([N4,1,1,1][Tf_2N]) and methyltrioctylammonium bis(trifluoromethylsulfonyl)imide ([N1,8,8,8][Tf_2N]). The solubility was determined on the basis of measuring phase boundaries, i.e., bubble point pressures, for a mixture of CO_2 and ionic liquid with a known composition at a fixed temperature. From the phase boundary data of the binary mixture, the CO_2 solubilities were obtained as a function of temperature and pressure. Moreover, the experimental data for the binary systems of CO_2+ionic liquids were correlated using the Peng-Robinson equation of state with the two adjustable binary interaction parameters in its mixing rules.

EXPERIMENTAL

1. Materials

Two ionic liquids ([N4,1,1,1][Tf_2N] and [N1,8,8,8][Tf_2N]) used in this work were purchased from Sigma-Aldrich. For solubility measurements, the ionic liquid sample was placed in the equilibrium cell, followed by evacuation using a mechanical pump at room temperature during several days. The analysis of coulometric Karl Fischer titration (Metrohm model 684) was performed to measure the water content for the evacuated ionic liquid samples. The characteristic values of the ionic liquids studied in this work are given in

†To whom correspondence should be addressed.
E-mail: bclee@hnu.kr

Table 1. Ionic liquids studied in this work

Chemical name	Abbreviation	Chemical formula	CAS number	Molecular mass	Purity (mass %)	Water content (mass %)
Butyltrimethylammonium bis(trifluoromethylsulfonyl)imide	[N4,1,1,1][Tf_2N]	$C_9H_{18}N_2S_2O_4F_6$	258273-75-5	396.37	98.5	0.40
Methyltrioctylammonium bis(trifluoromethylsulfonyl)imide	[N1,8,8,8][Tf_2N]	$C_{27}H_{54}N_2S_2O_4F_6$	375395-33-8	648.85	99	0.37

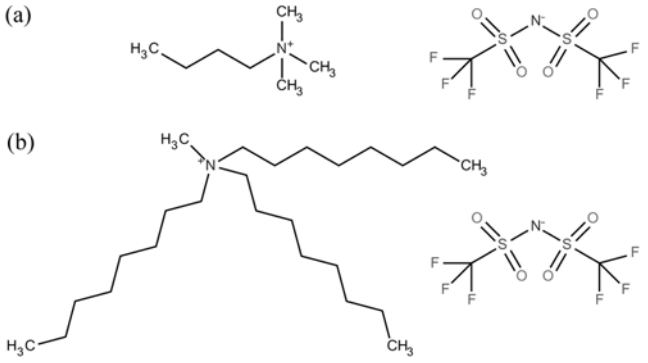

Fig. 1. Chemical structures of ionic liquids studied in this work: (a) [N4,1,1,1][Tf_2N]; (b) [N1,8,8,8][Tf_2N].

Table 1, and their chemical structures are shown in Fig. 1. CO_2 with 99.99% high purity to be used for measurements was purchased from Myung Sin General Gas Co. (Korea). No further purification was performed for use of the ionic liquids and CO_2.

2. Apparatus and Procedure

A high-pressure variable-volume view cell apparatus was set up for measuring the solubility of CO_2 in ionic liquids. A schematic diagram of the experimental apparatus and a detailed description of the experimental procedure are given in our previous publications [14,16,17]. The apparatus is composed of a view cell equipped with a sapphire window and a movable piston, a pressure generator (High Pressure Equipment Co. model 50-6-15), a borescope (Olympus model R080-044-000-50), a magnetic stirring system, and an air bath. The cylindrical view cell is 16 mm i.d. by 70 mm o.d., and its internal working volume is approximately 31 cm^3. A high-precision pressure gauge (Dresser Heise model CC-12-G-A-02B, ±0.05 MPa accuracy, ±0.01 MPa resolution) was used to measure the system pressure. An RTD probe inserted into the cell was used in measurement of the system temperature within ±0.1 K.

CO_2 solubilities in ionic liquid were determined through measuring bubble point pressures for CO_2+ionic liquid mixtures with various compositions at known temperatures. A feature of using the variable-volume view cell apparatus is that the concentration of the system is maintained constant throughout the experiment. A brief description of the experimental procedure is as follows. An ionic liquid sample was injected into the cell by using a gas-tight syringe. A sensitive balance (AND model HM-30) measurable to ±0.1 mg was used in determining the amount of the ionic liquid loaded. The cell was placed within the air bath after assembling a piston and a sapphire window. And then the cell was evacuated with a mechanical pump at room temperature during overnight to remove any entrapped air inside the cell and any dissolved gas and water in the ionic liquid.

CO_2 was delivered to the cell via a feed line by a small CO_2 cylinder after the vapor space of the cell was fully evacuated. The exact amount of CO_2 delivered to the cell was determined by measuring the weights of the CO_2 cylinder before and after delivery, in use of a balance (Precisa model 1,212 M) with an accuracy of ±1 mg. Through dipping the CO_2 cylinder in a Dewar flask full of liquid nitrogen, CO_2 gas in the feed line was recovered back into the CO_2 cylinder. For ionic liquid and CO_2, uncertainties in measuring their masses were 0.2 mg and 2 mg, respectively. For composition of each component, an uncertainty analysis was performed according to the ISO guideline [25].

For a CO_2+ionic liquid mixture with a specified overall composition, the system pressure was changed until the phase change inside the cell was visually observed through the cell window. The fluid in the cell was compressed to dissolve CO_2 into the ionic liquid. The fluid was well stirred and simultaneously heated to the target temperature. The system temperature was controlled within an uncertainty of ±0.1 K. At an elevated pressure, the fluid became a single homogeneous phase after dissolution of CO_2 into the ionic liquid phase. Then the pressure slowly decreased until tiny CO_2 bubbles started to form from the single phase solution. We defined the bubble point pressure of the solution at a given composition and temperature to be the initial pressure at which the first bubbles were observed. Every observation was repeated at least twice to ensure the reproducibility of experimental data. The uncertainty in measuring the bubble point pressure was 0.02 MPa. For a solution of very high CO_2 mole fractions, the cloud point behavior rather than the bubble point behavior was observed. Due to the phase transition from a single phase to a liquid+liquid phase, the solution became cloudy at the cloud point. The cloud pressure was defined as the pressure at which there was no more possibility of visually observing the stirring bar in the cell [26]. The precision for the measurement of cloud pressure was estimated to be about 0.1 MPa. Exactly the same way was repeated to measure the bubble or cloud point pressures at different temperatures and compositions.

CORRELATION

The solubility data for binary systems obtained in this work were correlated with a thermodynamic model which can be incorporated into a mathematical model for design calculation of absorption column. The correlation starts with a setup of phase equilibrium criterion for a binary system of CO_2 (component 1)+ionic liquid (component 2). Only pure CO_2 exists in the gas phase, because the ionic liquid is assumed to be non-volatile. Thus, the criterion for phase equilibrium at a constant temperature and pressure is satisfied when the fugacity of CO_2 in gas phase (f_1^{gas}) is equal to that of CO_2 in ionic liquid phase ($\hat{f}_1^{IL}$):

$$f_1^{gas} = \hat{f}_1^{IL} \quad (1)$$

The fugacity relationship with respect to temperature and pressure can be expressed by an equation of state. Among a variety of equations of state, the Peng-Robinson equation of state (PR-EoS), one of the most popular for practical applications, was used in this work.

The PR-EoS is written as follows [27]:

$$P = \frac{RT}{V-b} - \frac{a(T)}{V(V+b)+b(V-b)} \quad (2)$$

The following quadratic mixing rules were used to calculate the mixture parameters in ionic liquid phase:

$$a = \sum_i \sum_j x_i x_j a_{ij} \quad (3)$$

$$a_{ij} = (a_{ii}a_{jj})^{1/2}(1-k_{ij}) \quad (4)$$

$$b = \sum_i \sum_j x_i x_j b_{ij} \quad (5)$$

$$b_{ij} = \left(\frac{b_i + b_j}{2}\right)(1-l_{ij}) \quad (6)$$

In Eq. (5), $b_{ii}=b_i$ and $b_{jj}=b_j$. k_{ij} and l_{ij} in Eq. (4) and Eq. (6) are the binary interaction parameters. The EoS parameters for pure component i (a_{ii} and b_i) are the same as described in textbooks of classical thermodynamics [27]. The expressions for the fugacities of CO_2 in gas and ionic liquid phases using the PR-EoS can also be easily found from textbooks. Thus, it is not necessary to show the equations for calculating the pure component EoS parameters and the fugacities.

The utilization of the PR-EoS requires information on the critical properties and acentric factor for each component of the binary system. Those properties are readily available for CO_2, while they are not available for ionic liquids. Therefore, those properties for ionic liquids should be estimated. We used the modified Lydersen-Joback-Reid group contribution method proposed by Valderrama and Rojas [28] to estimate the critical temperature and pressure and the acentric factor of the ionic liquids studied. The estimated values of the properties for the ionic liquids studied in this work are given in Table 2 along with those for CO_2.

The phase equilibrium calculation for the CO_2+ionic liquid system was performed in the following way. At a given temperature, equilibrium pressures (P) satisfying Eq. (1) were calculated as a function of CO_2 mole fraction (x_1). The volumetric properties of CO_2 and ionic liquid phases, which were required to calculate f_1^{gas} and $\hat{f}_1^{IL}$, were obtained by solving Eq. (2). A nonlinear least square method was used to perform this calculation. The same calculations were repeated at different temperatures.

A set of the optimum values of k_{12} and l_{12} at each temperature for a binary system was determined first before performing the above phase equilibrium calculation. Those values were obtained by correlating the experimental $P-x_1$ data with the PR-EoS and minimizing the following objective function:

$$F = \sum_{m=1}^{N} \frac{\left|P_m^{calc} - P_m^{exp}\right|}{P_m^{exp}} \quad (7)$$

where P_m^{exp} is the experimental value of equilibrium pressure for data point m, P_m^{calc} is the equilibrium pressure calculated by the PR-EoS at the experimental value of x_1 for the same data point, and N is the number of data points. An optimization routine, which solved a nonlinear least-squares problem, was used.

Table 2. Critical properties and acentric factor estimated for ionic liquids

Ionic liquid	Critical temperature, T_c (K)	Critical pressure, P_c (MPa)	Critical compressibility factor, Z_c	Acentric factor, ω
[N4,1,1,1][Tf_2N]	1038.7	2.59	0.286	0.333
[N1,8,8,8][Tf_2N]	1376.1	1.06	0.184	0.996
CO_2	304.2	7.38	0.274	0.224

RESULTS AND DISCUSSION

1. CO_2 Solubility in Ionic Liquids

Solubility of gases including CO_2 in liquids tends to increase in proportion to pressure or decrease in inverse proportion to temperature. This tendency is universally applied to most ionic liquids reliant on physical absorption [11-22]. Even in chemical absorption with a strong CO_2 absorption capacity, dependence on physical absorption appears after absorption of a certain amount of CO_2. Our study for ammonium-based ionic liquids confirmed this trend as well. Tables 3 and 4 show the experimental results of the phase boundaries for two binary systems: CO_2+[N4,1,1,1][Tf_2N] and CO_2+[N1,8,8,8][Tf_2N], respectively. In those tables, the equilibrium pressure data observed at the bubble or cloud point of the CO_2 (component 1)+ ionic liquid (component 2) mixtures with different CO_2 mole fractions are given in the temperature range from about 303 K to about 343 K. The solubility data are provided in terms of the mole fraction

Table 3. Experimental bubble or cloud point data for various mole fractions of CO_2 in the CO_2+[N4,1,1,1][Tf_2N] system

Mole fraction of CO_2, x_1	Uncertainty in x_1	Molality, m_1 (mol of CO_2/kg of ionic liquid)	T (K)	P (MPa)	Phase behavior observed
0.0776	0.0016	0.2122	303.2	0.10	b[a]
			312.5	0.15	b
			322.5	0.20	b
			331.9	0.25	b
			342.3	0.35	b
0.1501	0.0029	0.4457	302.6	0.35	b
			312.4	0.45	b
			322.5	0.55	b
			332.7	0.75	b
			343.3	0.90	b
0.2554	0.0039	0.8655	302.7	0.95	b
			313.1	1.25	b
			322.9	1.50	b
			332.5	1.75	b
			342.8	2.10	b
0.3348	0.0048	1.2699	303.0	1.55	b
			312.0	1.85	b
			322.5	2.25	b
			332.9	2.65	b
			342.8	3.15	b

Table 3. Continued

Mole fraction of CO_2, x_1	Uncertainty in x_1	Molality, m_1 (mol of CO_2/kg of ionic liquid)	T (K)	P (MPa)	Phase behavior observed
0.4015	0.0055	1.6927	302.7	2.05	b
			313.1	2.50	b
			323.1	3.00	b
			333.9	3.65	b
			342.5	4.15	b
0.4825	0.0059	2.3521	302.5	2.80	b
			312.6	3.40	b
			322.5	4.15	b
			332.9	5.00	b
			342.8	5.80	b
0.5410	0.0063	2.9734	303.9	3.50	b
			313.4	4.30	b
			323.2	5.20	b
			332.7	6.20	b
			342.9	7.30	b
0.5851	0.0066	3.5580	303.2	4.15	b
			313.4	5.20	b
			323.4	6.30	b
			332.9	7.50	b
			342.9	8.95	b
0.6338	0.0067	4.3669	303.0	5.00	b
			314.9	6.50	b
			323.0	7.70	b
			332.6	9.35	b
			342.4	11.30	b
0.6711	0.0068	5.1469	303.0	5.75	b
			313.7	7.45	b
			322.8	9.30	b
			332.7	11.80	b
			342.5	14.55	b
0.7298	0.0063	6.8152	302.9	9.35	c[b]
			313.7	14.55	c
			322.6	18.80	c
			332.2	23.10	c
			342.5	27.45	c
0.7575	0.0062	7.8806	302.6	18.55	c
			313.2	24.30	c
			324.1	29.80	c
			333.1	34.00	c
			342.6	38.20	c
0.7802	0.0062	8.9537	303.1	33.10	c
			313.5	38.85	c
			322.8	43.55	c
			332.4	48.20	c
			342.8	52.80	c

[a]Bubble point behavior observed
[b]Cloud point behavior observed

of CO_2 (x_1) in the ionic liquid phase. The uncertainty in the solubility measurement is also given for each point. The average uncertainty

Table 4. Experimental bubble or cloud point data for various mole fractions of CO_2 in the CO_2+[N1,8,8,8][Tf_2N] system

Mole fraction of CO_2, x_1	Uncertainty in x_1	Molality, m_1 (mol of CO_2/kg of ionic liquid)	T (K)	P (MPa)	Phase behavior observed
0.2066	0.0037	0.4014	303.6	0.35	b[a]
			313.7	0.50	b
			323.5	0.60	b
			333.0	0.75	b
			342.7	0.85	b
0.3362	0.0063	0.7806	304.9	1.10	b
			314.2	1.25	b
			323.4	1.45	b
			332.8	1.65	b
			342.9	1.90	b
0.4309	0.0084	1.1672	303.7	1.55	b
			314.0	1.90	b
			323.6	2.20	b
			332.5	2.45	b
			343.0	2.85	b
0.4996	0.0101	1.5390	304.1	2.10	b
			314.0	2.50	b
			323.5	2.90	b
			333.1	3.35	b
			342.5	3.75	b
0.5535	0.0115	1.9108	303.2	2.60	b
			312.8	3.10	b
			323.6	3.65	b
			332.7	4.15	b
			342.8	4.75	b
0.5785	0.0132	2.1152	303.5	2.80	b
			313.9	3.35	b
			323.0	3.80	b
			333.0	4.40	b
			342.4	4.95	b
0.6413	0.0135	2.7554	303.0	3.45	b
			314.1	4.15	b
			323.9	4.85	b
			332.7	5.50	b
			343.3	6.30	b
0.6840	0.0138	3.3365	302.9	4.10	b
			313.9	4.95	b
			324.0	5.85	b
			333.1	6.65	b
			342.3	7.55	b
0.7174	0.0141	3.9127	303.4	4.65	b
			314.3	5.75	b
			323.5	6.65	b
			333.1	7.70	b
			342.7	8.80	b
0.7448	0.0144	4.4987	302.9	5.15	b
			314.0	6.30	b
			322.7	7.40	b
			332.9	8.70	b
			342.9	10.05	b

Table 4. Continued

Mole fraction of CO_2, x_1	Uncertainty in x_1	Molality, m_1 (mol of CO_2/kg of ionic liquid)	T (K)	P (MPa)	Phase behavior observed
0.7770	0.0140	5.3704	303.0	5.75	b
			313.9	7.25	b
			323.5	8.70	b
			333.1	10.30	b
			342.8	11.95	b
0.8074	0.0134	6.4588	302.7	6.40	b
			313.1	8.25	b
			323.4	10.45	b
			333.4	12.75	b
			342.4	14.75	b
0.8389	0.0124	8.0273	305.1	10.65	c[b]
			314.8	13.50	c
			323.4	15.70	c
			332.9	18.10	c
			343.0	20.60	c
0.8539	0.0122	9.0098	303.2	14.45	c
			312.8	16.60	c
			322.6	18.90	c
			332.6	21.40	c
			342.6	23.80	c
0.8667	0.0120	10.0218	303.2	19.00	c
			313.9	20.90	c
			323.4	22.85	c
			333.6	25.15	c
			342.6	27.10	c
0.8809	0.0115	11.3982	303.1	28.85	c
			314.3	28.90	c
			324.0	29.90	c
			333.2	31.45	c
			342.6	33.05	c

[a]Bubble point behavior observed
[b]Cloud point behavior observed

value in x_1 was estimated to be 0.0054 for the CO_2+[N4,1,1,1][Tf_2N] system and 0.0115 for the CO_2+[N1,8,8,8][Tf_2N] system.

For each data point, information on the phase change behavior observed during measurement, i.e., bubble or cloud point behavior, is also given in Tables 3 and 4. As indicated in the tables, the cloud point behavior rather than the bubble point behavior was observed for solutions of quite high CO_2 mole fractions: more than about 0.73 for the CO_2+[N4,1,1,1][Tf_2N] system and 0.84 for the CO_2+[N1,8,8,8][Tf_2N] system. This phenomenon can be explained in the following manner, as already discussed in our previous publication [15]. When the CO_2 solubility in ionic liquid is measured in our experiments, the pressure is slowly reduced until phase separation occurs from the single-phase solution where CO_2 is dissolved in the ionic liquid phase. When the CO_2 mole fraction in the solution is small and the equilibrium pressure is low, CO_2 behaves like a gas, and thus the tiny bubbles come out of the solution with the pressure decrease even at temperatures above the critical point of CO_2. However, at higher CO_2 mole fractions and higher pressure, CO_2 behaves like a liquid, and the cloud pressure behavior is observed with a decrease of the equilibrium pressure. It is acknowledged that the high density of the CO_2 phase makes the demixing appear closer to liquid-liquid equilibrium behavior than to vapor-liquid equilibrium behavior. Due to the phase transition from a single phase to a liquid+liquid phase, the solution becomes cloudy at the cloud point. The cloud point behavior was observed when the sharp increase of equilibrium pressure with the increase of CO_2 solubility occurred.

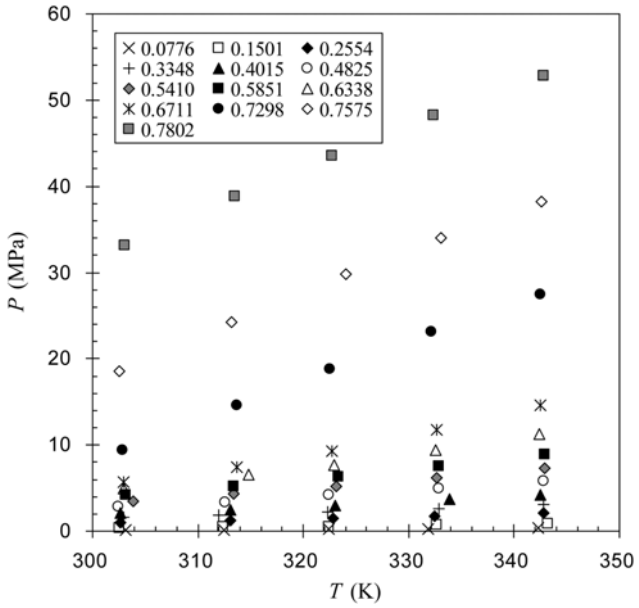

Fig. 2. P−T isopleths of phase boundaries for the CO_2+[N4,1,1,1][Tf_2N] mixtures with various CO_2 mole fractions (x_1).

As an example of the graphical presentation of the experimental data, the P−T isopleths for the CO_2+[N4,1,1,1][Tf_2N] system are shown in Fig. 2. As the temperature increased at a given CO_2 mole fraction, the equilibrium pressure increased. The change of the equilibrium pressure with respect to temperature increased with the increase of the CO_2 mole fraction. The equilibrium pressure increased significantly when the CO_2 mole fraction increased isothermally. This phenomenon can be more distinctly observed from a P−x_1 isotherm generated by plotting P as a function of x_1 at various temperatures. For this purpose, first, the P−T curves like Fig. 2 were fitted with polynomial equations (second- or third-order) to obtain the curve fits. And then the equilibrium pressures equivalent to desired temperatures were calculated from the curve fits. Finally, the equilibrium pressures (P) as a function of x_1 at different temperatures were obtained for each system. The interpolated isothermal P−x_1 data obtained from the curve fits are listed in Table 5 for two systems. Fig. 3 is a graphical illustration of the P−x_1 isothermal data for the CO_2+[N1,8,8,8][Tf_2N] system. In Fig. 3, the solubilities of CO_2 in mole fraction for [N1,8,8,8][Tf_2N] are shown as a function of pressure at several temperatures.

The equilibrium pressure was relatively low at lower CO_2 compositions, while it increased sharply at higher CO_2 compositions. For example, in case of the CO_2+[N1,8,8,8][Tf_2N] in Fig. 3, the equilibrium pressure gradually increased until the CO_2 mole fraction reached about 0.8. On the other hand, at the CO_2 mole fractions higher

Table 5. Interpolated isothermal solubility data for CO_2 in ionic liquids

Mole fraction of CO_2, x_1	Molality, m_1 (mol of CO_2/kg of ionic liquid)	P (MPa) at following temperature				
		303.2 K	313.2 K	323.2 K	333.2 K	343.2 K
Ionic liquid: [N4,1,1,1][Tf_2N]						
0.0776	0.2122	0.10	0.15	0.20	0.27	0.35
0.1501	0.4457	0.35	0.46	0.58	0.73	0.91
0.2554	0.8655	0.97	1.23	1.51	1.80	2.10
0.3348	1.2699	1.56	1.89	2.27	2.69	3.16
0.4015	1.6927	2.07	2.51	3.02	3.58	4.21
0.4825	2.3521	2.83	3.48	4.20	4.99	5.85
0.5410	2.9734	3.44	4.28	5.21	6.23	7.34
0.5851	3.5580	4.16	5.15	6.28	7.56	8.98
0.6338	4.3669	5.03	6.25	7.74	9.47	11.46
0.6711	5.1469	5.77	7.37	9.41	11.88	14.79
0.7298	6.8152	9.48	14.37	19.05	23.51	27.76
0.7575	7.8806	18.89	24.29	29.35	34.07	38.44
0.7802	8.9537	33.17	38.66	43.79	48.56	52.97
Ionic liquid: [N1,8,8,8][Tf_2N]						
0.2066	0.4014	0.35	0.48	0.61	0.74	0.86
0.3362	0.7806	1.07	1.24	1.44	1.66	1.91
0.4309	1.1672	1.55	1.86	2.18	2.51	2.84
0.4996	1.5390	2.06	2.47	2.90	3.34	3.79
0.5535	1.9108	2.61	3.11	3.63	4.19	4.77
0.5785	2.1152	2.79	3.30	3.83	4.40	5.00
0.6413	2.7554	3.46	4.11	4.80	5.53	6.30
0.6840	3.3365	4.12	4.91	5.76	6.67	7.64
0.7174	3.9127	4.64	5.61	6.64	7.72	8.85
0.7448	4.4987	5.16	6.25	7.44	8.72	10.10
0.7770	5.3704	5.77	7.16	8.66	10.29	12.03
0.8074	6.4588	6.45	8.35	10.41	12.62	14.99
0.8389	8.0273	10.13	12.98	15.67	18.22	20.62
0.8539	9.0098	14.43	16.72	19.07	21.49	23.98
0.8667	10.0218	18.97	20.82	22.82	24.98	27.28
0.8809	11.3982	28.78	29.00	29.82	31.25	33.29

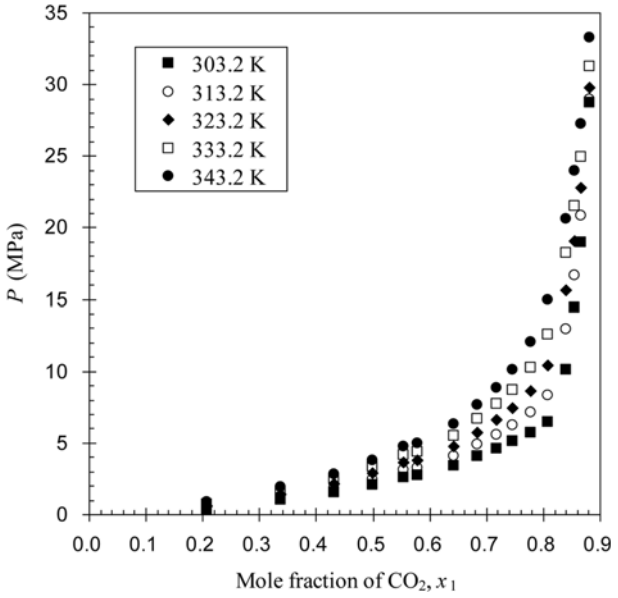

Fig. 3. P–x_1 diagrams of the CO_2+[N1,8,8,8][Tf_2N] mixtures at different temperatures.

than about 0.8, the equilibrium pressure increased very sharply even with a small increase of the CO_2 mole fraction. This tendency was also generally observed for other ionic liquids as well as [N4,1,1,1][Tf_2N], to a greater or lesser extent [11-14,16-21]. Consequently, as the ionic liquids subject to this study basically show the phenomenon of physical absorption with regard to CO_2, they have limitations in that the equilibrium pressure rapidly increases at a certain CO_2 mole fraction or higher. The higher CO_2 absorption capacity the ionic liquids have, the higher CO_2 mole fraction where the rapid change in equilibrium pressure is observed. As seen in Fig. 3, the CO_2 solubility decreased with an isobaric increase in temperature. In addition, its larger temperature dependence was observed at higher CO_2 mole fractions.

Fig. 4 compares the CO_2 solubility data for two ionic liquids [N4,1,1,1][Tf_2N] and [N1,8,8,8][Tf_2N] at 323.15 K. The CO_2 solubilities in ionic liquid were compared with respect to both the mole fraction and the molality. It illustrates the effect of structural modification of ammonium in the cation on the CO_2 solubility for the [Tf_2N] anion-based ionic liquids. Compared at the same temperature and pressure, [N1,8,8,8][Tf_2N] had a higher CO_2 solubility than [N4,1,1,1][Tf_2N]. This phenomenon can be explained in the fol-

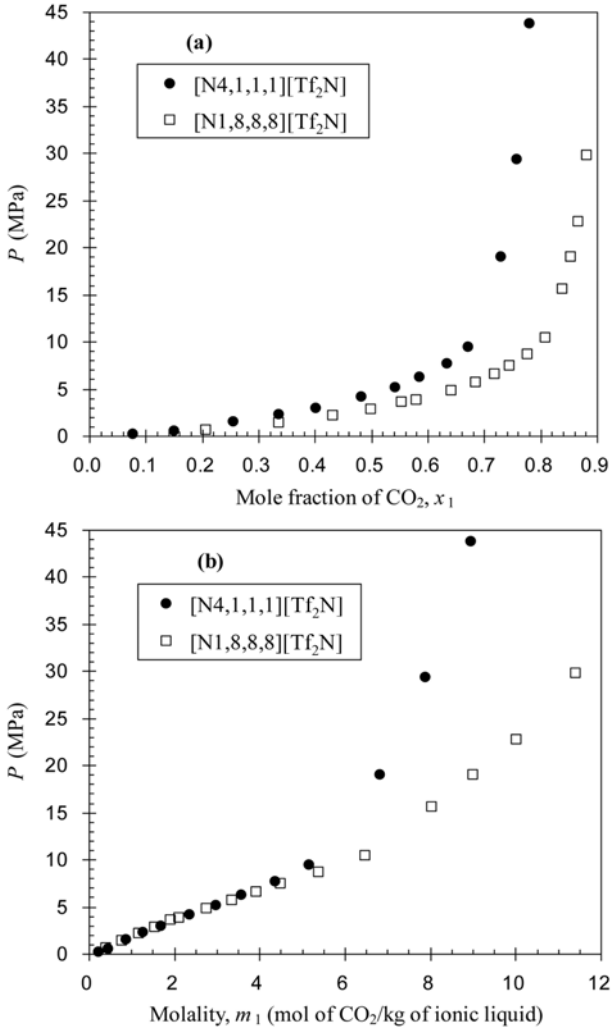

Fig. 4. Comparison of CO_2 solubility in ionic liquids [N4,1,1,1][Tf_2N] and [N1,8,8,8][Tf_2N] at 333.2 K: (a) solubility in mole fraction; (b) solubility in molality.

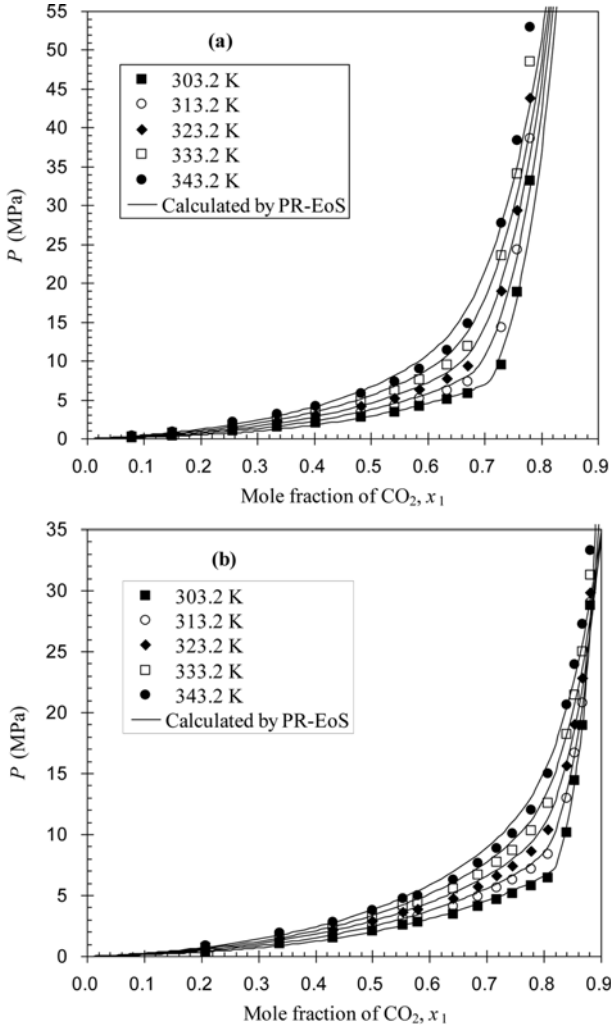

Fig. 5. Comparison between experimental values and calculated results by the PR-EoS for CO_2 solubility in ionic liquids: (a) [N4,1,1,1][Tf_2N]; (b) [N1,8,8,8][Tf_2N].

lowing manner. As seen in the chemical structures of two ionic liquids (Fig. 1), the total length of the side chains attached to the ammonium cation of [N1,8,8,8][Tf_2N] is longer than that of [N4,1,1,1][Tf_2N]. It is assumed that the longer side chains can expand free volume and increase CO_2 absorbed in the space [12]. As for another factor, the longer alkyl chain, the more weakened combination between cation and anion and the stronger combination between cation and CO_2, and it led to increase in CO_2 absorption [29]. Consequently, the CO_2 solubility in ionic liquids increased with increase of the total length of alkyl chains attached to the ammonium cation of the ionic liquids, and this increase became more apparent at higher pressures. In Fig. 4(b), the CO_2 solubility results in [N4,1,1,1][Tf_2N] and [N1,8,8,8][Tf_2N] are illustrated in terms of the molality instead of the mole fraction. Unlike the mole fraction data, the molality data showed a little different behavior. As shown in Fig. 4(a), [N1,8,8,8][Tf_2N] always gave higher CO_2 solubilities in the mole fraction than [N4,1,1,1][Tf_2N] in the whole range of pressure. On the other hand, until the pressure reached about 8 MPa, the molality values of CO_2 in [N4,1,1,1][Tf_2N] and [N1,8,8,8][Tf_2N] were almost the same. This can be attributed to the big difference in molecular masses of two ionic liquids. At pressures higher than about 8 MPa, the molality of CO_2 in [N1,8,8,8][Tf_2N] was larger than that in [N4,1,1,1][Tf_2N], and the difference between two values became much bigger as the pressure increased. The same trends were also found at other temperatures. Therefore, when comparing the solubility of a gas in ionic liquids, it is necessary to express the gas solubility in terms of the molality as well as the mole fraction. This is because there may be a big difference in the molecular masses of ionic liquids depending on the types of cation and anion constituting the ionic liquids.

2. Correlation Results

The PR-EoS using the quadratic mixing rules was used to correlate the experimental data of the solubility of CO_2 in the ionic liquids studied in this work. For each system of CO_2+ionic liquid, the two binary interaction parameters (k_{12} and l_{12}) in the mixing rules were optimized using the P−x_1 data given in Table 5. Table 6 lists the optimum values of the k_{12} and l_{12} parameters at five different temperatures for each system. The calculated results are graphically presented in Fig. 5 along with the experimentally obtained data of Table 5. The correlation results are summarized in Table 6. The average absolute deviations in percentage (AAD%) between the calculated and ex-

Table 6. Binary interaction parameters and correlation results using the PR-EoS for the CO_2+ionic liquid systems

Ionic liquid	T (K)	Binary interaction parameters		AAD%[a]
		k_{12}	l_{12}	
[N4,1,1,1][Tf_2N]	303.2	0.10210	0.08261	11.3
	313.2	0.10357	0.07743	9.9
	323.2	0.10530	0.07554	9.5
	333.2	0.10605	0.07257	9.1
	343.2	0.10712	0.07009	8.6
[N1,8,8,8][Tf_2N]	303.2	0.03985	0.03222	4.8
	313.2	0.03778	0.03122	4.8
	323.2	0.03523	0.03109	5.8
	333.2	0.03242	0.03132	6.5
	343.2	0.02970	0.03190	6.9

[a]Average absolute deviation in percentage, which is defined as:

$$AAD\% = \frac{1}{N}\sum_{m=1}^{N}\frac{|P_m^{calc} - P_m^{exp}|}{P_m^{exp}} \times 100 \quad \text{(N: number of data)}$$

perimental equilibrium pressures were calculated at five temperatures for each system. The average value of AAD% for entire data points in the whole range of temperature was 9.7% for [N4,1,1,1][Tf_2N] and 5.8% for [N1,8,8,8][Tf_2N], respectively. The CO_2+[N1,8,8,8][Tf_2N] system gave a little better correlation result. Overall, it can be concluded that the PR-EoS can satisfactorily correlate the high-pressure solubility of CO_2 in [N4,1,1,1][Tf_2N] and [N1,8,8,8][Tf_2N] with the AAD% less than 10% over a wide range of pressure up to the supercritical region of CO_2.

CONCLUSIONS

For the two types of ammonium-based ionic liquids with different lengths of side chains in their cation, their solubilities of CO_2 were determined by measuring the bubble or cloud point pressures of the binary mixtures of CO_2+ionic liquid using a high-pressure equilibrium apparatus equipped with a variable-volume view cell. Very high solubilities were obtained in the ionic liquids at lower pressures, whereas a sharp increase in the equilibrium pressure was observed at higher CO_2 compositions. The variation of the length of alkyl chains attached to the ammonium cation had a considerable effect on the CO_2 solubility in ionic liquid. The CO_2 solubility increased with an increase in the length of total alkyl chains on the cation at low pressures, and this increase became more apparent at higher pressures. The solubility data of CO_2 in the ammonium-based ionic liquids could be successfully correlated by using the PR-EoS with the AAD% of less than 10% over a wide range of pressure up to the supercritical region of CO_2.

ACKNOWLEDGEMENT

This research was supported by Basic Science Research Program through the National Research Foundation of Korea (NRF) funded by the Ministry of Education, Science and Technology (grant number 2011-0013925) and by the 2012 Research Fund of Hannam University.

REFERENCES

1. R. Sheldon, *Chem. Commun.*, 2399 (2001).
2. W. Xu and C. A. Angell, *Science*, **302**, 422 (2003).
3. R. P. Swatloski, S. K. Spear, J. D. Holbrey and R. D. Rogers, *J. Am. Chem. Soc.*, **124**, 4974 (2002).
4. L. A. Blanchard, D. Hancu, E. J. Beckmanm and J. F. Brennecke, *Nature*, **399**, 28 (1999).
5. S. K. Jeong, D. H. Kim, I. H. Baek and S. H. Lee, *Korean Chem. Eng. Res.*, **46**, 492 (2008).
6. J. E. Bara, T. K. Carlisle, C. J. Gabriel, D. Camper, A. Finotello, D. L. Gin and R. D. Noble, *Ind. Eng. Chem. Res.*, **48**, 2739 (2009).
7. M. H. Cho, H. Lee and H. Kim, *Korean Chem. Eng. Res.*, **48**, 1 (2010).
8. J. F. Brenneke and B. E. Gurkan, *J. Phys. Chem. Lett.*, **1**, 3459 (2010).
9. M. B. Shiflett, A. M. Niehaus and A. Yokozeki, *J. Chem. Eng. Data*, **55**, 4785 (2010).
10. D. D. Iarikov, P. Hacarlioglu and S. T. Oyama, *Chem. Eng. J.*, **166**, 401 (2011).
11. A. Shariati and C. J. Peters, *J. Supercrit. Fluids*, **30**, 139 (2004).
12. S. N. V. K. Aki, B. R. Mellein, E. M. Saurer and J. F. Brennecke, *J. Phys. Chem. B*, **108**, 20355 (2004).
13. M. Kroon, A. Shariati, M. Costantini, J. van Spronsen, G.-J. Witkamp, R. A. Sheldon and C. J. Peters, *J. Chem. Eng. Data*, **50**, 173 (2005).
14. D.-J. Oh and B.-C. Lee, *Korean J. Chem. Eng.*, **23**, 800 (2006).
15. J. L. Anderson, J. K. Dixon and J. F. Brennecke, *Acc. Chem. Res.*, **40**, 1208 (2007).
16. E.-K. Shin, B.-C. Lee and J. S. Lim, *J. Supercrit. Fluids*, **45**, 282 (2008).
17. E.-K. Shin and B.-C. Lee, *J. Chem. Eng. Data*, **53**, 2728 (2008).
18. B.-H. Lim, W.-H. Choe, J.-J. Shim, C. S. Ra, D. Tuma, H. Lee and C. S. Lee, *Korean J. Chem. Eng.*, **26**, 1130 (2009).
19. P. J. Carvalho, V. H. Alvarez, I. M. Marrucho, M. Aznar and J. A. P. Coutinho, *J. Supercrit. Fluids*, **52**, 258 (2010).
20. J.-H. Yim, H. N. Song, B.-C. Lee and J. S. Lim, *Fluid Phase Equilib.*, **308**, 147 (2011).
21. J.-H. Yim, H. N. Song, K. P. Yoo and J. S. Lim, *J. Chem. Eng. Data*, **56**, 1197 (2011).
22. Y. R. Jin, Y. H. Jung, S. J. Park and I. H. Baek, *Korean Chem. Eng. Res.*, **50**, 35 (2012).
23. D. M. D'Alessandro, B. Smit and J. R. Long, *Angew. Chem. Int. Ed.*, **49**, 6058 (2010).
24. M. B. Shiflett, D. W. Drew, R. A. Cantini and A. Yokozeki, *Energy Fuels*, **24**, 5781 (2010).
25. *Guide to the expression of uncertainty in measurement*, International Organization of Standardization (ISO), Geneva, Switzerland (1995).
26. J. M. Lee, B.-C. Lee and S.-H. Lee, *J. Chem. Eng. Data*, **45**, 851 (2000).
27. J. M. Prausnitz, R. N. Lichtenthaler and E. G. de Azevedo, *Molecular thermodynamics of fluid-phase equilibria*, 3rd Ed., Prentice-Hall, NJ, USA (1999).
28. J. O. Valderrama and R. E. Rojas, *Ind. Eng. Chem. Res.*, **48**, 6890 (2009).
29. R. E. Baltus, B. H. Culbertson, S. Dai, H. Luo and D. W. DePaoli, *J. Phys. Chem. B*, **108**, 721 (2004).